NASA/TM–20210026743

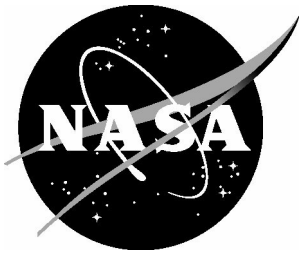

Development of Advanced Manufacturing Approaches for Single-Piece Launch Vehicle Structures

Wesley A. Tayon
Langley Research Center, Hampton, Virginia

Michelle T. Rudd
Marshall Space Flight Center, Huntsville, Alabama

Marcia S. Domack
Langley Research Center, Hampton, Virginia

Mark W. Hilburger
Langley Research Center, Hampton, Virginia

January 2022

NASA STI Program Report Series

Since its founding, NASA has been dedicated to the advancement of aeronautics and space science. The NASA scientific and technical information (STI) program plays a key part in helping NASA maintain this important role.

The NASA STI program operates under the auspices of the Agency Chief Information Officer. It collects, organizes, provides for archiving, and disseminates NASA's STI. The NASA STI program provides access to the NTRS Registered and its public interface, the NASA Technical Reports Server, thus providing one of the largest collections of aeronautical and space science STI in the world. Results are published in both non-NASA channels and by NASA in the NASA STI Report Series, which includes the following report types:

- TECHNICAL PUBLICATION. Reports of completed research or a major significant phase of research that present the results of NASA Programs and include extensive data or theoretical analysis. Includes compilations of significant scientific and technical data and information deemed to be of continuing reference value. NASA counterpart of peer-reviewed formal professional papers but has less stringent limitations on manuscript length and extent of graphic presentations.

- TECHNICAL MEMORANDUM. Scientific and technical findings that are preliminary or of specialized interest, e.g., quick release reports, working papers, and bibliographies that contain minimal annotation. Does not contain extensive analysis.

- CONTRACTOR REPORT. Scientific and technical findings by NASA-sponsored contractors and grantees.

- CONFERENCE PUBLICATION. Collected papers from scientific and technical conferences, symposia, seminars, or other meetings sponsored or co-sponsored by NASA.

- SPECIAL PUBLICATION. Scientific, technical, or historical information from NASA programs, projects, and missions, often concerned with subjects having substantial public interest.

- TECHNICAL TRANSLATION. English-language translations of foreign scientific and technical material pertinent to NASA's mission.

Specialized services also include organizing and publishing research results, distributing specialized research announcements and feeds, providing information desk and personal search support, and enabling data exchange services.

For more information about the NASA STI program, see the following:

- Access the NASA STI program home page at http://www.sti.nasa.gov

- Help desk contact information:

https://www.sti.nasa.gov/sti-contact-form/
and select the "General" help request type.

NASA/TM–20200026743

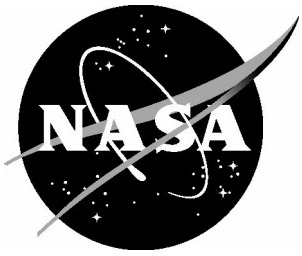

Development of Advanced Manufacturing Approaches for Single-Piece Launch Vehicle Structures

Wesley A. Tayon
Langley Research Center, Hampton, Virginia

Michelle T. Rudd
Marshall Space Flight Center, Huntsville, Alabama

Marcia S. Domack
Langley Research Center, Hampton, Virginia

Mark W. Hilburger
Langley Research Center, Hampton, Virginia

National Aeronautics and
Space Administration

Langley Research Center
Hampton, Virginia 23681-2199

January 2022

National Aeronautics and
Space Administration

Langley Research Center
Hampton, Virginia 23681-2199

January 2022

Available from:

NASA STI Program / Mail Stop 148
NASA Langley Research Center
Hampton, VA 23681-2199
Fax: 757-864-6500

Abstract

Advanced, near-net shape manufacturing methods have the potential to enable production of structures with fewer welds and reduced machining requirements. Two such methods that are suitable for the manufacturing of single-piece, stiffened barrel-shaped structures are presented. The first solution deployed existing manufacturing technology to produce a thick-walled barrel with integrally machined stiffeners. In this study, an 8-ft. diameter barrel was produced and subjected to a buckling test. Data on the manufacturing and testing of this barrel are provided and compared against the traditional multi-piece weld construction approach. The single-piece barrel resulted in a 28% greater load carrying capacity than the welded barrel.

A second solution utilized a novel flow-forming technique to produce the barrel and stiffeners in one process without the need for welding or machining. This is an emerging manufacturing method known as the Integrally Stiffened Cylinder (ISC) process. This innovative process is being evaluated for launch vehicle and commercial aircraft manufacturing. The one-piece, stiffened ISC barrels, which have been successfully fabricated at 10 ft. in diameter, offer a direct replacement for conventional multi-piece, welded or riveted structures. A cost-benefit analysis for launch vehicle cryogenic propellant tanks estimated that the ISC process offers up to a 50 % reduction in manufacturing costs and a 10 % reduction in mass.

1. Introduction

In the 1950s and 1960s, human-rated launch vehicles in the United States were developed to send NASA astronauts to the Moon, thereby fulfilling President Kennedy's promise to land an American on the Moon by the end of the 1960s. Little has changed in the design and manufacture of the core launch vehicle structure over the past 5 decades of US-led human spaceflight, despite the emergence of innovative manufacturing methods. Incumbent fabrication techniques for metallic launch vehicle structures, such as propellant tanks, inter-stages and adapters, comprise multi-piece welded and/or riveted construction methods synonymous with the Apollo era. Production typically involves the use of thick-plate starting stock, which is machined into monocoque structures incorporating skin-stringer, ortho- or iso-grid stiffeners. Current manufacturing and design options tend to negatively impact system architecture.

An example of such deficiencies is demonstrated in an assessment of the 27.5-ft. diameter Space Shuttle External Tank (ET) assembly that is still considered state-of-the-art. The ET assembly consisted of liquid oxygen and liquid hydrogen cryogenic tanks and an intertank structure. The barrel sections of both the liquid oxygen and hydrogen tanks were fabricated from stiffened panel segments that were integrally-machined from 2-inch thick flat Al-Li alloy plate, bump-formed to the required curvature, and welded together. Machining resulted in material waste of approximately ~500,000 lbs. of chips, or ~ $8M in raw material waste, for each ET [1]. The liquid oxygen tank required 4 panels and the liquid hydrogen tanks required 8 panels per barrel segment. After machining and bump forming, each of these panels were longitudinally welded together to form a barrel section. Approximately 1/8 of a mile (7,200 inches) of longitudinal welds were required to assemble the barrel sections. Circumferential welds joined several barrel sections and two end domes to complete the tank, totaling roughly 3/8 of a mile of circumferential welds per tank.

The ET fabrication practice represents the baseline for NASA's new vehicle, the Space Launch System (SLS). There are two aspects of this multi-piece construction that result in significant debits to performance and cost: machining and welding. Eliminating or minimizing the requirement to machine from thick plate starting material enables greener manufacturing and more efficient material utilization, serving to decrease both cost and manufacturing time. The combination of longitudinal and circumferential welds sum to ~ ½ a mile of welds that have to be meticulously inspected prior to flight and pose the greatest risk of catastrophic failure within the tank structure, contributing to high labor costs and increased manufacturing cost and time. In addition, the weld regions suffer from mechanical property knockdown, requiring additional thickness in the welded areas (commonly referred to as weld lands) to compensate for a loss in strength. This leads to a parasitic weight increase of roughly 5% [2].

Previous structural testing and analysis studies performed under NASA's Shell Buckling Knockdown Factor (SBKF) project have concluded that stiffness and geometric discontinuities associated with longitudinal weld lands in compression loaded cylinders can reduce the buckling load of the multi-piece, welded barrels [3]. Localized geometric imperfections occur in the barrel, magnifying the inherent imperfection sensitivity due to factors associated with the welding process. Therefore, it is anticipated that seamless barrel fabrication technologies can improve structural efficiency by eliminating these weld-related issues. Additional weight savings beyond the 5% associated with eliminating increased gages in the weld lands are attainable through redesign that takes advantage of the increased structural efficiency.

A viable solution to counter the issues highlighted above is to replace multi-piece with single-piece construction ideology. Single-piece manufacturing methods offer the potential to reduce both mass and cost concurrently. These are the key decision-making factors influencing vehicle design and mission operations. Mass savings for launch vehicle structures enables larger

payloads, while lower manufacturing costs reduce the payload price-per-pound to orbit. Cryogenic fuel tanks represent a significant fraction of the dry mass of launch vehicles, offering an opportunity for infusion of new manufacturing solutions. The application of innovative manufacturing processes will enable more economically and structurally efficient tank production.

Recently, NASA has explored two single-piece manufacturing approaches for barrel sections used in cryogenic fuel tanks in attempts to reduce mass and cost. The two approaches utilize an advanced manufacturing technology known as flow-forming. In flow-forming, an initial thick-wall ring is formed between opposing rollers. The rollers translate in the longitudinal direction to thin the wall of the ring and simultaneously elongating the ring into a barrel. The first approach is to produce a cylinder with a thick wall from which an internal stiffener geometry can be machined post-flow-forming. Existing manufacturing technology enables this option to be implemented using commercially-available equipment with minimal effort. This approach eliminates the need for longitudinal welding, but still requires extensive machining.

The second approach exploits a novel concept, known as flow-forming, to simultaneously form a thin-walled barrel with internal stiffeners in one processing step. This process has been pioneered by researchers at NASA Langley Research Center (LaRC) and is referred to as the Integrally Stiffened Cylinder (ISC) Process. The ISC process eliminates the need for longitudinal welding and also minimizes machining required to achieve final geometry. Currently, this approach will require additional development in order to commercialize the process. Initial developments have successfully demonstrated the concept with good repeatability at a commercially-relevant scale. Both approaches will be discussed in subsequent sections, by detailing the processes and including relevant test data.

Both NASA and US commercial launch companies will greatly benefit from the development and commercialization of the single-piece, advanced manufacturing approaches. Within NASA, the development of single-piece structures is extremely relevant to the following Space Technology Mission Directorate (STMD) Strategic Thrusts (STs): “ST2. Enable Safe and Efficient Transport into and Through Space,” and “ST6. Grow and Utilize the U.S. Industrial and Academic Base” [4]. This work falls under the “Advanced Materials” STMD key technology focus area. Development of the Integrally Stiffened Cylinder Process was specifically highlighted in the NASA FY19 Budget Estimate under “Exploration Research and Technology” for Advanced Materials (referred to as the Advanced Near Net Shape Technology, or ANNST, within section ERT-22) [5].

The proposed technologies will decrease launch vehicle costs for new missions to cis-lunar space, the Moon, and Mars. NASA will rely heavily on commercial launch partners to accomplish this work; hence more near-term application may reside in commercial crew launch vehicles. Beyond launch vehicle applications, single-piece stiffened cylinders have many other potential applications. These include habitat structures for the Moon and Mars (either through repurposing of launch vehicles structures or as separate dedicated hardware), missiles and rocket applications within the Department of Defense, aircraft fuselage structures (currently being explored through the NASA Aeronautics Mission Directorate), drilling shafts for mining and oil and gas industries, submarines and submersible vehicles, and for ground-based transportation systems (trains, mass transit vehicles, Hyperloop).

2. Commercially-Available Technology – Flow-Formed and Machined Barrels

2.1 Manufacturing Process Description

Single-piece, thick, smooth-walled cylinders are commercially-available products with multiple potential US vendors capable of producing such cylinders. ATI Ladish Forgings (now known as ATI Forged Products) produced two seamless Al 2219 flow-formed barrels under contract to NASA in support of the SBKF project. A barrel is shown at various stages of the forming sequence in Figure 1. Each barrel was formed from a starting cylindrical ingot (Figure 1(a)) of just over 8,000 lbs. The ingot was upset forged to increase the diameter, leading to a shorter, wider cylinder. Subsequently, the workpiece was pierced to produce a hollow cylinder to facilitate the next step of saddle rolling. During saddle rolling, the workpiece was worked to expand the diameter of the hole to an inner diameter that was sufficiently large to enable ring rolling. During ring rolling, the diameter was further expanded as the wall thickness was reduced. Ring rolling continued until the target diameter was reached. Machining after ring rolling was performed to clean up the surface (Figure 1(b)). During final flow-forming, the ring was lengthened as the wall thickness was further reduced with the diameter remaining constant (Figure 1(c)).

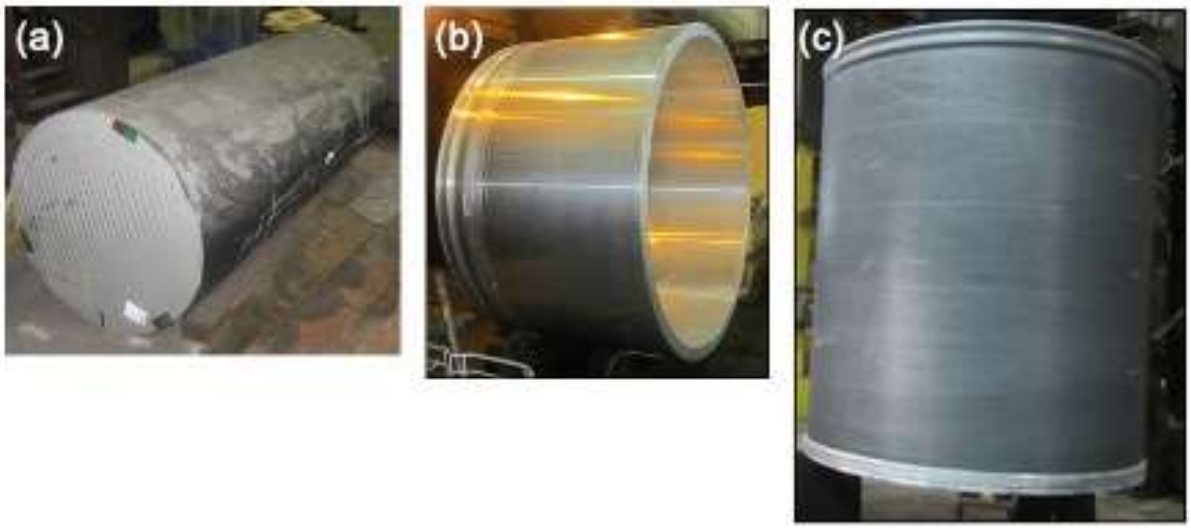

Figure 1. Forming sequence for seamless barrel fabrication; (a), cylindrical ingot; (b), ring-rolled and machined hollow cylinder; (c), 96.5 in. diameter flow-formed barrel.

The flow-formed cylinders were solution heat treated at 995 ± 10°F for 2.5 hours and then quenched in a drop-bottom furnace. After solution treatment, the cylinders were cold stretched a proprietary amount based on diametral expansion prior to artificial aging at 350 ± 10°F for 18 hours. The final dimensions of the cylinders were as follows: outside diameter of 96.5 inches, length of 90 inches, and a wall thickness of 2.5 inches. These thick-wall cylinders were delivered to NASA in the T851 temper condition.

2.2 Mechanical Properties

Each cylinder included a trim ring on one end that was removed after heat treatment and cut into arc segments for mechanical property testing at ATI Ladish Forgings, NASA Marshall Space Flight Center (MSFC) and NASA LaRC. Testing included tensile, compression, and fracture

toughness, in axial (A), circumferential (C), and radial (R) orientations at both ambient (72°F) and cryogenic (-320°F) temperatures according to the test matrix shown in Table 1 with specified orientations in Figure 2. Results were consistent between cylinders, arc segments, and between test labs. Tensile, compression, and fracture toughness properties averaged for both cylinders and all test laboratories are shown for each orientation in Table 2, Table 3, and Table 4. Handbook values are shown at the bottom of each Table for comparison.

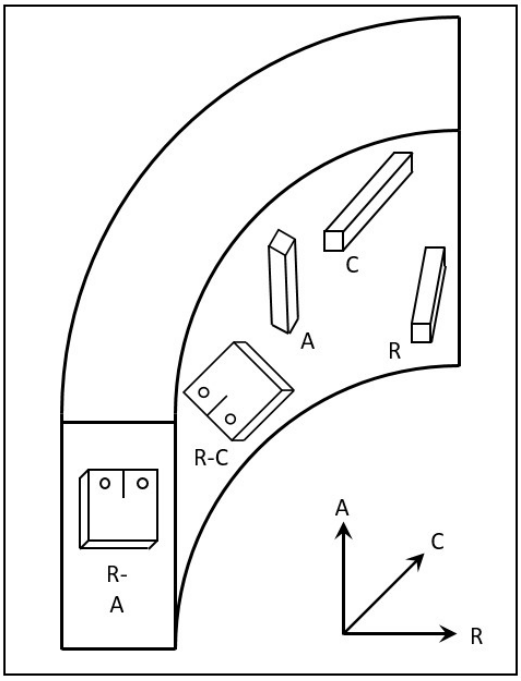

Figure 2. Specimen orientation for thick-wall flow-formed barrel.

Table 1. Mechanical property test matrix.

Test	Orientation	Temperature
Tensile	A, C, R	RT, -320°F
Compression	A, C, R	RT
Fracture Toughness	A-C, C-A, R-A, R-C	RT, -320°F

Table 2. Average tensile properties.

Test Lab	Test Temp (°F)	Orientation	UTS (ksi)	YS (ksi)	El (%)	E (Msi)
Avg All	72	A	65.9	49.9	10.2	10.7
		C	65.6	50.6	11.5	10.5
		R	58.3	50.9	2.1	10.6
MSFC	-320	A	82.2	60.4	11.6	11.3
		C	83.4	62.3	12.9	10.7
		R	69.0	58.5	2.2	11.4
Hand Forgings and Rolled Rings [6], [7]	RT	A	58.0	46.0	6.0	10.6
		C	60.0	48.0	4.0	
		R	58.0	44.0	3.0	
T851 Sheet and Plate [6], [8]	RT	L / T	62	45	6	10.6
	Cryo	L	100	63	12	11.8

Tensile and yield strengths were isotropic for A and C orientations, with values agreeing within 3%. Strengths were lower for the R orientation by up to 15%. Elongation values were within 5% for A and C orientations, but considerably lower for the R orientation. Tensile properties were comparable to handbook values for wrought products with strength values in A and C orientations within 1% for rolled plate and elongations values within 2% of rolled plate [6–8]. Tensile strengths and elastic modulus exhibited the expected increase at cryogenic temperature. Modulus increased by 5-12% for each orientation. Yield and ultimate strengths increased by over 20% for each orientation.

Table 3. Average compressive properties.

Test Lab	Test Temp (°F)	Orientation	CYS (ksi)	Ec (Msi)
Avg All	72	A	51.5	10.7
		C	50.8	10.7
		R	51.7	10.6
Sheet and Plate [6], [9]		L	53	10.8
		T	54	10.8

Compression properties measured at ambient temperature were uniform between cylinders and arc segments and comparable to handbook properties. The compression yield strength (CYS) was isotropic within 2% and the compression modulus (E_c) was isotropic within 1%. The CYS of the cylinders was within 3% of typical values for plate, comparing axial data for the cylinder with longitudinal data for plate, and within 6% for circumferential cylinder data compared with transverse plate data [6]. The E_c was within 1% of typical values for plate [9].

Table 4. Fracture toughness properties.

Test Lab	Test Temp (°F)	Orientation	J_Q (in-lbs/in^2)	K_{Jq} (ksi-in$^{1/2}$)	Valid
LaRC/MSFC	72	A-C	85.8	31.9	N
LaRC	72	C-A	111.5	36.1	N
MSFC	-320	A-C	107.6	36.7	N
		C-A	125.6	39.7	N
		R-A	47.9	24.5	N
		R-C	51.4	26.0	N
Typical K_{Ic} - T851 plate Specified minimum at RT [10]		L-T	-	24	-
		T-L	-	20	-
		S-L	-	18	-

Fracture toughness values, indicated by K_{Jq}, were highest in all cases for the C-A orientation, over the A-C orientation by 12% at room temperature and 8% at cryogenic temperature. Values for the R-A and R-C orientation at cryogenic temperature were lower by about 30% compared with A-C and C-A orientations. The expected increase at cryogenic temperature was observed and was higher by 15% and 10% for A-C and C-A orientations, respectively. K_{Jq} values were higher than handbook K_{Ic} values for plate by 10% to 40% when compared with L-T and T-L orientations [10]. All fracture toughness tests were invalid due to crack tunneling.

2.3 Seamless barrel test article (STA8.1)

NASA MSFC was responsible for machining the thick-wall cylinders to yield a thin-walled, orthogrid stiffened cylinder, referred to as STA8.1, for structural testing under the SBKF project. The starting 2.50-inch wall thickness provided a sufficient envelope for machining to account for any out of roundness in the part due to the flow-forming process. The outer mold line (OML) was machined to a final diameter of 96.00 inches. An orthogrid pattern was machined into the inner mold line (IML) of the cylinder using a 7-axis milling machine, as shown in Figure 3. To perform stiffener machining, the cylinder was laid on its side and secured in place using a custom vacuum chuck. Since there were no weld lands, 145 longitudinal stiffeners were evenly spaced at 2.482-degrees around the circumference of the cylinder, and the circumferential ribs had an axial spacing of 5.064 in. The longitudinal and circumferential stiffeners were designed to have the same nominal thickness of 0.065 in. The stiffeners had a nominal height of 0.570 in. as measured from the OML, and the nominal skin thickness was 0.070 in. At the ends of the cylinder, the axial stiffeners tapered into a transition section.

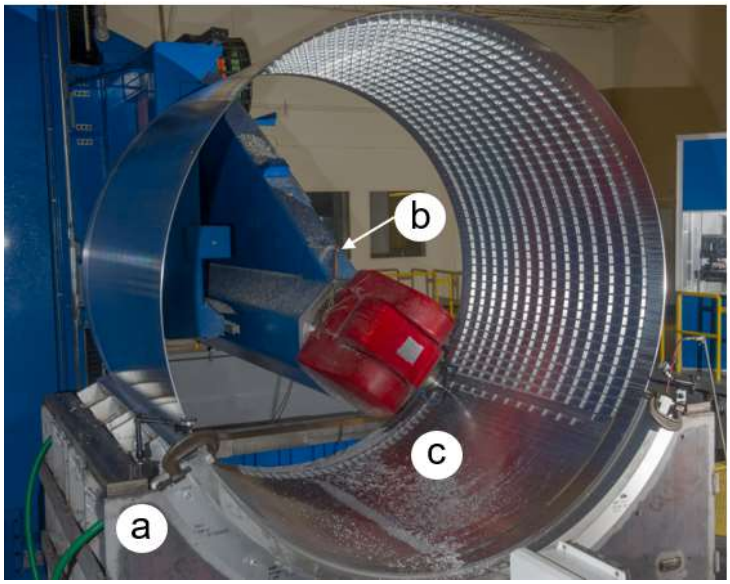

Figure 3. STA8.1 in the process of machining on the 7-axis milling machine: a, vacuum chuck; b, 7-axis milling machine; and c, machined test article.

2.4 Demonstrated benefits

A major benefit for building single-piece structures is the increase in load carrying capability due to removing weld lands. To better assess the effects of eliminating welded joints, the acreage of design of the seamless, machined test article (STA8.1) was based on an 8-ft-diameter test article, TA09, fabricated using the multi-piece, machined and welded approach that was previously tested by SBKF.

Both test articles had very similar stiffener spacings, and exactly the same skin thickness and stiffener height. Though the geometry was similar, STA8.1 and TA09 were made out of different aluminum alloys. Test article TA09 was an assembly of three Al-Li 2195 orthogrid-stiffened panels that were welded together using the friction stir welding process. The test article contained three longitudinal weld lands spaced 120-degrees apart around the circumference. STA8.1 was fabricated from a single Al 2219 thick-walled cylinder.

A critical factor in the prediction of buckling response are geometric imperfections in the test article prior to loading. Thus, the OML surfaces of both test articles were characterized using structured-light scanning to capture any imperfections associated with the fabrication of each test article. The OML radial imperfections from the manufacturing process for TA09 are presented in Figure 4. An interesting feature of the TA09 geometric imperfections was the distinct signature left behind from the welding process.

As seen in Figure 4, there were localized areas of inward (negative) deformation, the blue regions, located at each weld land location at 60°, 180°, and 300°. These areas were a result of shrinkage caused by the friction stir welding process. TA09 had a minimum inward radial displacement of 0.138-inch, and the maximum outward (positive) radial displacement was 0.104-inch; a peak-to-peak amplitude of 0.242-inch. In contrast, the STA8.1 geometric imperfection plot, Figure 5, does not have defined, localized areas of inward imperfections. For STA8.1 the maximum outward displacement was 0.056-inch, and the minimum inward displacement is 0.037-inch; peak-to-peak amplitude of 0.093-inch. The TA09 imperfection amplitude was more than double than the imperfection amplitude of STA8.1.

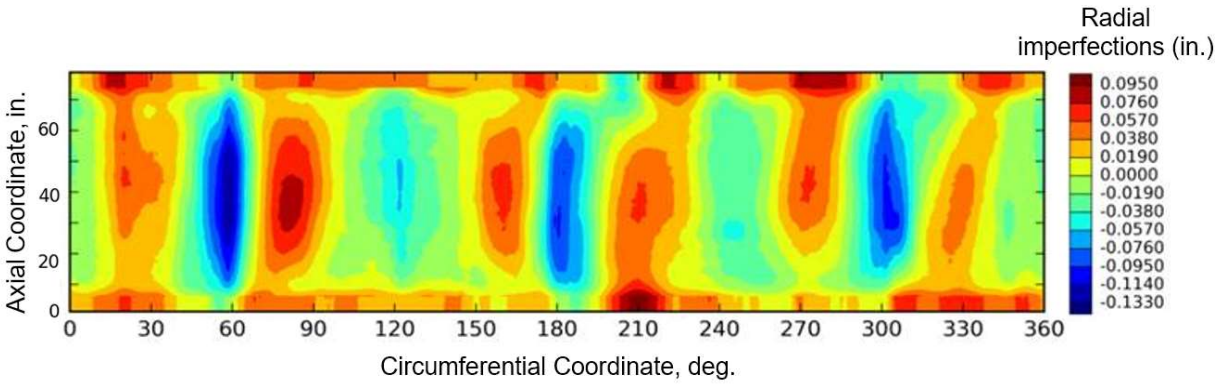

Figure 4. Test article TA09 measured radial imperfections.

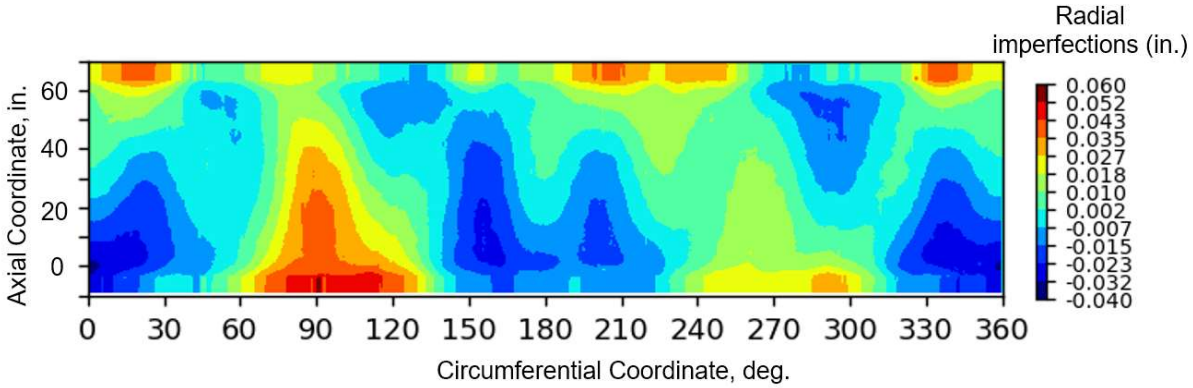

Figure 5. Test article STA8.1 measured radial imperfections.

A numerical comparison can be made between STA8.1 and TA09 to assess the effects of the geometric imperfections and weld lands because the acreage designs are similar. Initially, the nonlinear buckling load for TA09 without weld lands, and no geometric imperfections is 738,000 lbs. The nonlinear buckling load with weld lands and the TA09 measured geometric imperfections is 509,000 lbs. These results imply that the combination of the weld lands and the geometric imperfections caused by the welding process reduced the load carrying capability by 31%.

A nonlinear transient analysis was completed with TA09 nominal geometry with weld lands and no geometric imperfections to assess the effects of the weld lands alone. The analysis resulted in a buckling load of 585,000 lbs. This value compared to the 738,000 lbs. buckling load determined from the nonlinear transient analysis of TA09 with a uniform stiffness, i.e. without weld lands, indicates a 21% loss of load carrying capability due to the weld land geometry.

The effect of imperfections without the influence of weld lands can be evaluated by mapping the TA09 geometric imperfections onto a model of TA09 without weld lands. A nonlinear transient analysis of this model resulted in a buckling load of 646,000 lbs. Comparing this value to the perfect, uniform stiffness nonlinear buckling load of 738,000 lbs., the geometric imperfections contributed to an approximately 12% reduction in load carrying capability. Therefore, it can be concluded that weld lands are the primary contributor to the reduction in buckling load.

Nonlinear transient analyses of STA8.1, with and without geometric imperfections were performed to understand the effects of geometric imperfections on STA8.1. The buckling load of STA8.1 without geometric imperfections was 720,000 lbs. This value can be compared to the buckling load determined from a nonlinear transient analysis with the measured STA8.1 geometric imperfections, i.e. 697,000 lbs. These results show that the measured geometric imperfections reduced the buckling load for this specific acreage design by 3%. All loads are summarized in Table 5.

Table 5. Summary of analysis buckling loads from weld land geometric imperfection sensitivity study.

Analysis Details	STA8.1	TA09
Nonlinear transient w/o geometric imperfections w/o weld lands	720,000 lbs	738,000 lbs
Nonlinear transient w/o geometric imperfections w/weld lands	N/A	585,000 lbs
Nonlinear transient w/geometric imperfections w/o weld lands	697, 000 lbs	646,000 lbs
Nonlinear transient w/geometric imperfections w/weld lands	N/A	509,000 lbs

The contributions of the radial imperfections and the stiffness discontinuity from the presence of weld lands decreases load carrying capability significantly based on this analysis. The welding process resulted in the radial imperfections. Radial imperfections caused a 3% reduction in buckling load. The weld lands resulted in a 31% reduction in buckling load. It may be concluded from these findings that a 28% increase in load carrying capability can be achieved with this acreage design using seamless manufacturing techniques.

A detailed description of the test and analysis correlation of STA8.1 have been documented [2]. The elimination of welds, and in turn weld lands, results in a mass savings. It is noteworthy that the welded test article (TA09) was made from a lighter alloy with a higher elastic modulus, Al-Li alloy 2195. The seamless test article (STA8.1) was made from a heavier, lower-strength alloy, Al 2219. Al-Li alloy 2195 (ρ = 0.097 lbs/in^3) is roughly 5% lower density than Al 2219 (ρ = 0.103 lbs/in^3). In terms of raw mass, STA8.1 was approximately equivalent to TA09. However, the true mass savings for eliminating weld lands is 5% when accounting for the difference in density.

The seamless, machined cylinder eliminates the need for all longitudinal welding in comparison to the typical multi-piece, machined and welded construction. This enables a reduction in manufacturing schedule and cost associated with welding and inspection. As STA8.1 demonstrated, the removal of weld lands can save mass and significantly increase load carrying capability. However, a significant amount of machining is required to take the as-formed thick-wall cylinder to a thin-wall orthogrid stiffened barrel. The level of machining is likely on par with that of the multi-piece, machined and welded approach, but with the added complexity of having to machine on a curved surface. Tighter tolerances can be achieved in future endeavors with proper tooling based on lessons learned from machining of the seamless barrel. The next step is to build these structures near-net with minimal machining using the Integrally Stiffened Cylinder (ISC) process knowing the benefits of building grid-stiffened structures without weld lands.

3. Developmental Technology – Integrally Stiffened Cylinder (ISC) Process

3.1 ISC Process Description

The ISC process is a metal flow-forming operation, which creates integral longitudinal stiffeners on the inner mold line (IML) surface of a cylinder. During the process, a preform is flow-formed over a cylindrical mandrel, which has grooves machined on the outer mold line (OML) surface that correspond to the desired stiffener shape. The nature of the preform has varied from a disc to a thick-walled ring, depending on the scale and forming machine constraints – this will be detailed in Section 3.2. Both the mandrel and preform are spinning during forming. Forming occurs at room temperature with no active heating, but there is localized heating of the part due to friction. Forming is facilitated through external rollers that spin in the circumferential direction

and translate in the axial direction to provide the necessary mechanical force. Flow-forming offers two options or modes: forward or back flow-forming.

In forward flow-forming, the rollers move axially with the cylinder as it lengthens. Forming starts at the bottom of the preform / mandrel and progresses toward the top of the mandrel. This method requires a mandrel that is the same length as the desired final part as the rollers will have to translate the full axial length of the formed cylinder. The machine will also have to be large enough to allow for rollers to translate the full length of the part. Thus, forward flow-forming has the disadvantages of higher equipment and tooling costs. In back flow-forming, the rollers move opposite the direction of cylinder elongation. Forming starts at the top of the preform as the rollers translate down the part, forcing material to flow out of the mandrel into free space. In this case, the mandrel only needs to be some fraction of the final part length, offering reduced tooling costs. Likewise, the rollers are forming over a smaller region of the final part length, thereby enabling forming on a smaller machine.

3.2 ISC Historical Development

The ISC process development began with a successful proof of concept demonstration of an 8-inch diameter aluminum-lithium alloy 2195 cylinder in 2012 using a commercial automotive clutch housing flow-forming machine. The clutch housing forming machine utilized a disc-shaped preform, referred to as a forming blank, rather than a thick-wall cylinder as is the case for all subsequent forming activities. The parts were formed using the forward flow-forming approach. A depiction of the process is shown in Figure 6. The forming blank is positioned on top of the mandrel. The first step utilizes spin forming to bend the blank over the mandrel. In the second step, flow-forming is used to elongate and thin the blank and force material into the grooves on the mandrel to form the stiffeners.

Photos of the disc preform and a typical Al-Li 2195 clutch housing can be seen in Figure 7. The clutch housing demonstration had numerous, short (0.12-inch tall) gear teeth that were not representative of typical cryogenic tank stiffeners. Continued development occurred at that scale for two more years, leading to stiffener spacing and height to be more representative of cryogenic tank designs, while also examining the effect of groove shape on the efficiency of material fill and stiffener formation. At the 8-inch diameter scale, using a different mandrel design, stiffeners up to 0.75 inches tall were successfully produced as seen in the ISC alongside the clutch housing cylinder in Figure 7.

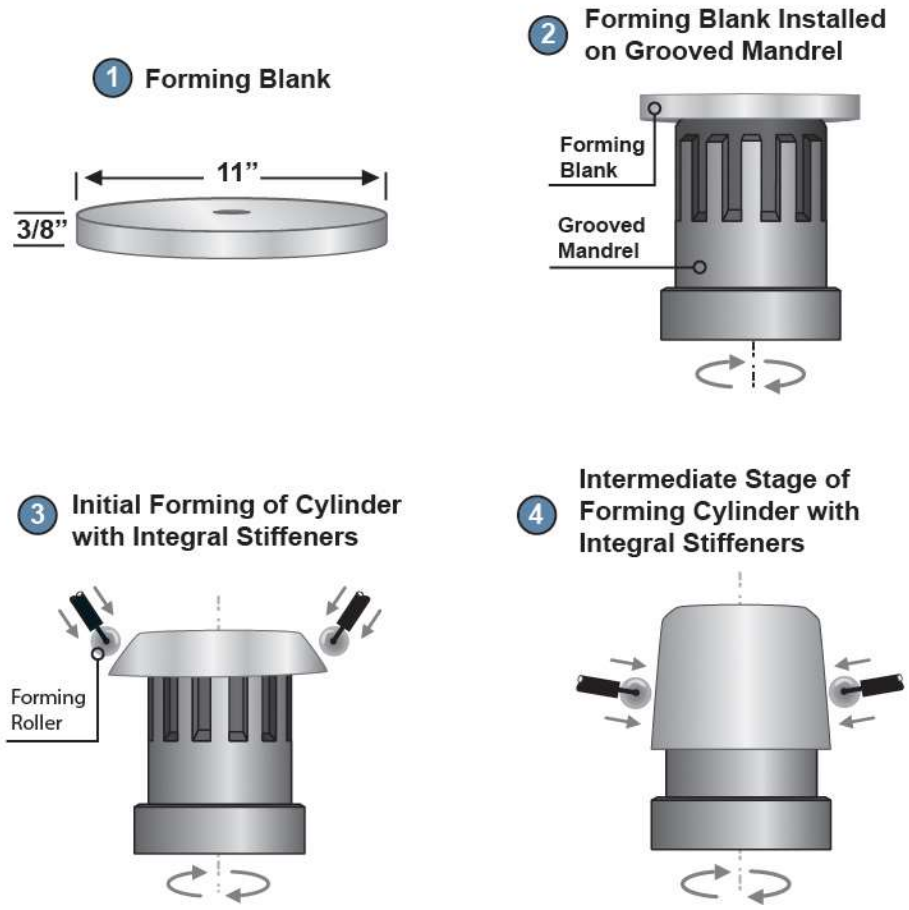

Figure 6. Subscale ISC forming process using automotive clutch housing machine.

Figure 7. Subscale, 8-inch diameter clutch housing (right), ISC (left) and preform disk (rear).

In 2014, the ISC project team embarked on ground and flight test campaign of ISC hardware. In 2015, the process was scaled up to a diameter of 17 inches, ultimately producing an ISC that was flown on a sounding rocket in collaboration with NASA Wallops Flight Facility. Once again,

forward flow-forming was implemented. In this case, the preform was a thick-walled cylinder. Successful scale-up, flight certification and demonstration of the ISC hardware on Sounding Rocket Flight 36.310 Hesh from Wallops Flight Facility on October 7, 2015, demonstrated the feasibility of the ISC process to efficiently manufacture launch vehicle hardware. One of the as-formed sounding rocket cylinders is shown in Figure 8. As a risk reduction effort to meet the flight schedule, the flight cylinder had 0.2-inch-tall stiffeners. In parallel with the flight campaign, additional forming trials were conducted and successfully demonstrated 1-inch-tall stiffeners at the sounding rocket scale (Figure 8).

Figure 8. Sounding rocket scale cylinders – as-formed sounding rocket cylinder (top) and segment from a 17-inch diameter cylinder with 1-inch tall stiffeners (inset).

3.3 Commercial-Scale Demonstration and Manufacturing

NASA and MT Aerospace embarked on a commercial scale manufacturing demonstration following the sounding rocket demonstration. The goal was to demonstrate the ISC process at a 10-ft. diameter scale, comparable in scale to many commercial launch vehicles and to the 8-ft. diameter demonstration of the seamless, thick-walled machined barrel. The Scot Forge Company (Spring Grove, IL) supplied preform rings for all the 10-ft. diameter ISC forming campaigns. A sequence of photos depicting the preform fabrication process are shown in Figure 9. The starting thick-walled preform was fabricated from a cylindrical shaped ingot. The ingot was initially upset forged and converted into a short and wide cylinder, while employing cross-forging techniques for microstructure control. Subsequently, the cylinder was pierced leaving a small hole through the center. This hole facilitates saddle rolling to expand the diameter. Once the diameter was opened to a sufficient size, the cylinder was ring rolled to the target outer diameter and wall thickness.

Subsequently, the rings are annealed to an O-temper condition, a common practice for aluminum alloys that follows protocols established in AMS 2770 [11]. The O-temper provided excellent ductility and low strength, representing a condition that is optimal for maximum formability. The ring was produced slightly oversized to facilitate machining of the preform to the necessary final dimensions. Typical final dimensions for the 10-ft. diameter preforms were 1.0-to-1.5-inch wall thickness, and 18-30 inches in height, and were similar to the rings shown in Figure 10. These dimensions were ultimately dictated by the desired final dimensions of the ISCs.

Figure 9. Preform fabrication process at Scot Forge.

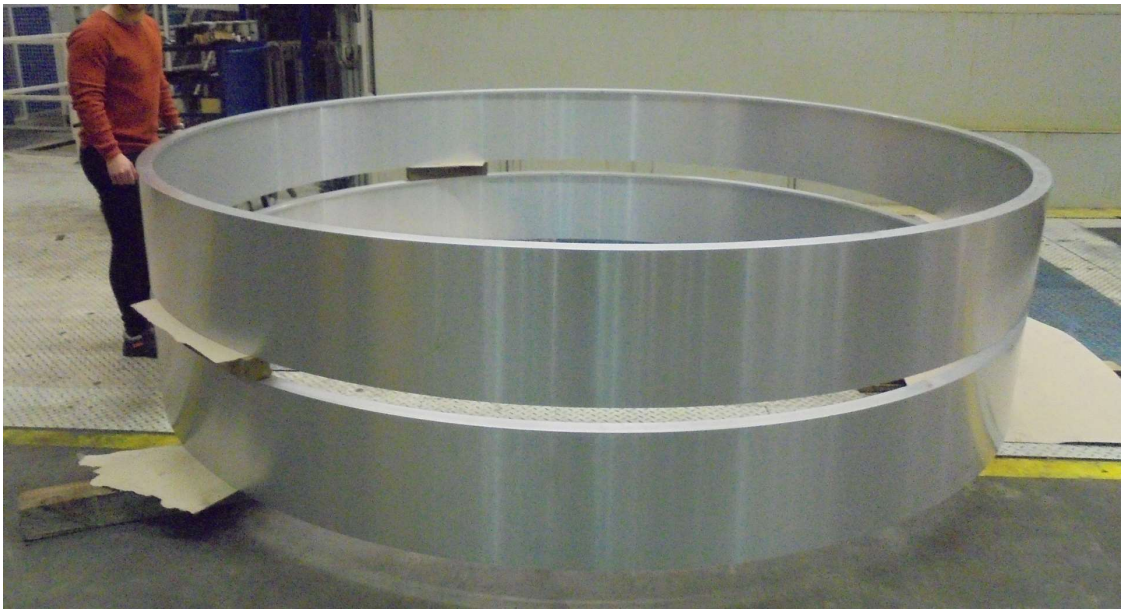

Figure 10. Example of two 10-ft. diameter aluminum ring preforms.

At the 10-ft. diameter scale, forming trials were conducted on an ESA-owned, commercial counter-roller flow-forming forming machine operated by MT Aerospace (Augsburg, Germany). This machine was designed for serial production of 10-ft. diameter, smooth-walled D6AC steel booster segments for the Ariane program without the use of a mandrel. Modifications to the roller geometry, forming parameters, and addition of a mandrel to the forming process enabled ISC forming on the booster production machine. ESA permitted NASA and MT Aerospace to conduct ISC forming trials on their commercial production equipment during negotiated production stoppages. ESA and MT Aerospace have also partnered separately to support forming trials for future ESA launch vehicle applications.

The machine operated in a backward flow-forming mode. It has four pairs of counter rollers equally spaced every 90° about the circumference of the part. The position of the rollers about the circumference was fixed, while the axial position of the rollers was staggered slightly and allowed to translate axially during the process. A thin-walled mandrel was introduced to facilitate stiffener forming that is specific to the ISC process depicted in Figure 11. The internal rollers provided support to the hollow mandrel and the external forming rollers exerted force against the outer wall of the preform. The latter extend the length of the cylinder and reduce the wall thickness, while simultaneously forcing material into the mandrel grooves to form the stiffeners. The number and geometry of the grooves in the mandrel can be tailored for the desired longitudinal stiffener configuration and spacing in the final part.

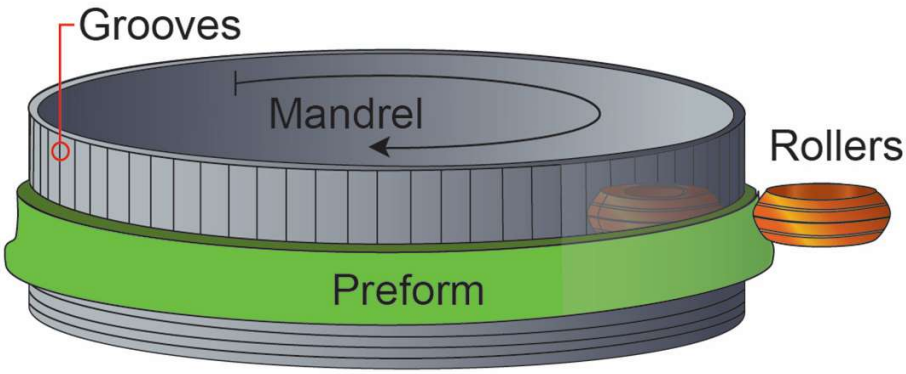

Figure 11. Depiction of the Integrally Stiffened Cylinder (ISC) Process.

The ISC forming mandrels were machined from a hollow, steel cylinder. OML surface grooves are machined according to the desired stiffener geometry. NASA explored forming with two different mandrels in separate 10-ft. diameter NASA forming campaigns occurring in 2017 and 2019. The two mandrels are shown in Figure 12. The 2017 mandrel had 48 stiffeners equating to a stiffener spacing of approximately 8 inches. A total of twelve unique stiffener geometries (combinations of 2 different shapes, 3 different depths, and 2 different widths) were used and repeat 4 times around the circumference. The details of the stiffener geometries can be found in [12].

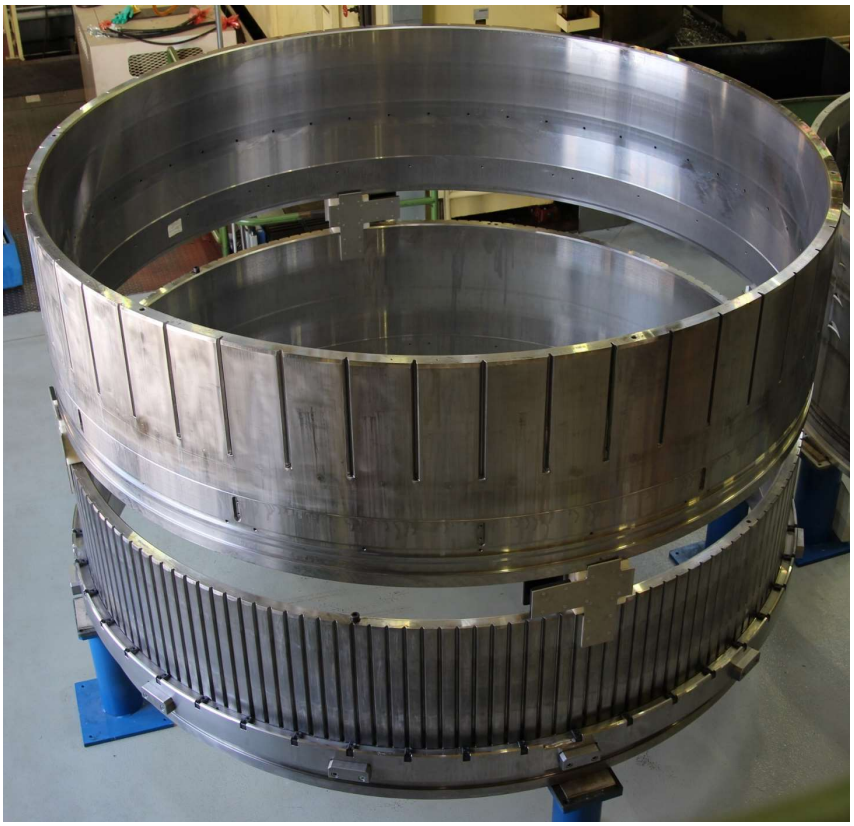

Figure 12. Two ISC forming mandrels with 48 stiffeners (top) from 2017 campaign, and 164 stiffeners (bottom) from 2019 campaign.

During the 2017 forming campaign, NASA and MT Aerospace successfully demonstrated the feasibility of manufacturing 10-ft. diameter ISCs. The campaign tallied a total of 7 forming trials.

Over the course of those trials, there was significant improvement in the process for both Al 2219 and Al-Li alloy 2050, which lead to the production of the ISC seen below in Figure 13. Unfortunately, none of the cylinders were produced without some degree of cracking within the stiffeners. NASA LaRC led material characterization and testing efforts to diagnose the cause of the cracking and determine materials processing improvements to eliminate its occurrence. Sections from multiple 2219 and 2050 10-ft. diameter ISCs were delivered to NASA LaRC to support these efforts. The NASA led study reported that a lack of ductility in the starting material, insufficient lubrication, and differential material flow between the wall and stiffeners all contributed to the cracking observed [12].

Figure 13. Successfully formed 10-ft. diameter ISC from 2017 forming campaign.

In response to the cracking witnessed during the 2017 campaign, modifications were undertaken to improve the manufacturing process to produce defect-free ISCs at the commercial scale. Modifications to the next generation mandrel included decreasing stiffener spacing and height, and adopting a uniform stiffener shape to minimize the differential flow rate. The mandrel used for the 2019 campaign had a total of 164 stiffeners with a spacing of approximately 2.3 inches (Figure 12). These stiffeners had the same geometry, depth (0.5 inches), and width (0.25 inches). Additional process modifications included improving the preform fixturing method to the mandrel to prevent slippage during forming, change of lubrication, and selection of Al 6061 (higher ductility and greater formability than 2219). The switch to Al 6061 was done primarily for risk reduction due to its inherently good formability and heritage in ISC development.

A total of 10, Al 6061 preform rings were supplied for forming trials. MT Aerospace experimented with > 20 forming parameters that led to improved forming and the production of multiple, defect-free ISCs, one of which is shown in Figure 14. A minimum wall thickness of ~ 1/8 inch (3 mm) was achieved and a maximum length of 5.2 ft. (1580 mm) was demonstrated. This represents a ~3x increase in length and a ~10x reduction in thickness from the starting preform dimensions. The typical forming time accounting solely for the time that the machine was actively forming the part was roughly 1.5 hours. Of the 10 attempts, 6 ISCs were produced of varying

lengths and wall thickness without any cracking and the stiffeners achieved full fill. Only 4 of the forming trials resulted in cracking, two of which were related to machine programming errors.

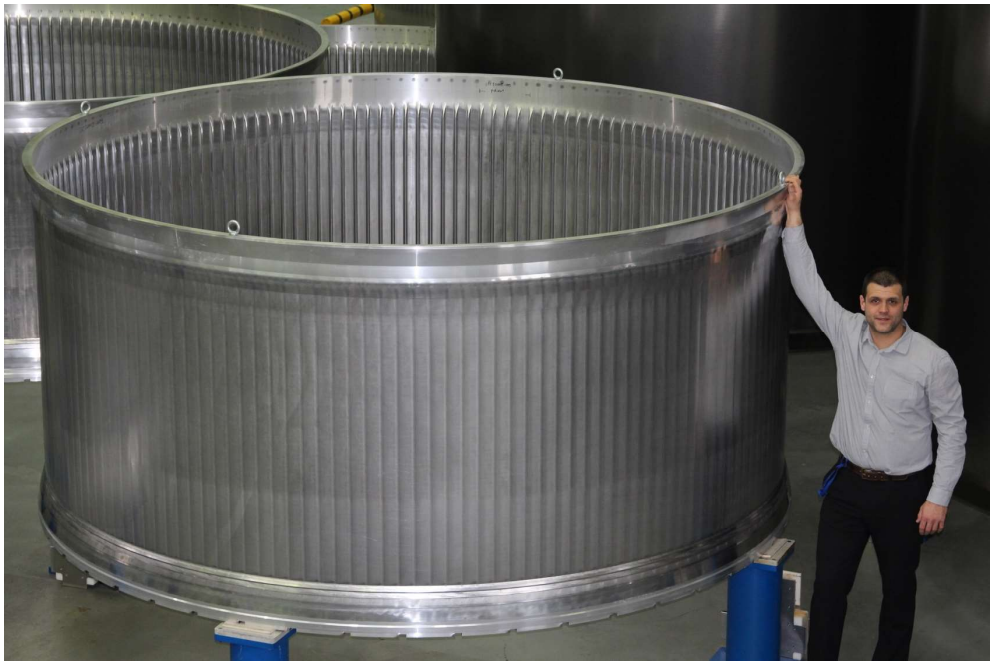

Figure 14. 10-ft. diameter Al 6061 ISC produced in 2019.

Over the course of the two forming campaigns, representing a total of 17 unique forming trials at the 10-ft. diameter scale, the ISC process was successfully demonstrated in the production of 10-ft. diameter stiffened cylinders in Al alloys 2219, 6061, and Al-Li alloy 2050. Continuous process improvements were made from lessons learned throughout those 17 trials. In the most recent campaign, 5 crack-free Al 6061 ISCs were manufactured with a maximum length of 5 ft., stiffener spacing of ~2.3 inches and a stiffener height of 0.5 inches. It is worth noting that the longitudinal stiffener spacing and stiffener height are almost identical to the longitudinal stiffeners from the seamless, machined barrel (STA8.1) discussed in Section 2.

A comparison of the manufacturing demonstrations from a decade of ISC process development, as described in the previous paragraphs, is summarized in Table 6 and includes cylinder diameter, stiffener height, number of stiffeners, stiffener spacing, and aluminum alloys investigated. These values do not necessarily represent limitations of the process, but bracket the physical dimensions that have been successfully explored.

Table 6. ISC process development and demonstrated dimensions.

Year	Diameter (inches)	Max Stiffener Height (inches)	Number of Stiffeners	Approximate Stiffener Spacing (inches)	Alloys Used
2012	8	0.12	42	0.6	Al-Li 2195
2013	8	0.75	6	4.2	Al-Li 2195 Al 6061
2015	17	1.0	6	8.9	Al 6061 Al 2219
2017	120	0.8	48	7.9	Al 2219 Al-Li 2050
2019	120	0.5	164	2.3	Al 6061

Beginning in 2019, NASA funded a third, 10-ft. diameter ISC manufacturing campaign to support the Advanced Air Transport Technology (AATT) project under the Aeronautics Research Mission Directorate (ARMD). The AATT project is developing technologies for ultra-efficient commercial aircraft. One objective of the project is to reduce assembly time and cost through rapid, net-shape forming of integrated structure and simultaneously reducing weight through elimination of fasteners. The AATT project is exploring the use of ISC technology to fabricate single-piece barrel sections for aircraft fuselages. Although the ISC approach can produce the required skin and a longitudinally stiffened structure, additional secondary structures are required. Secondary structures include circumferential ring frames, window belts, and door frames.

Accordingly, the ISC process will be combined with complementary manufacturing processes that can join and/or build up secondary structures on the pre-formed ISC. The intent is to demonstrate a novel metallic fuselage design and manufacturing processes at scale and rate. The goal is to attain a manufacturing rate of 100 aircraft per month, 10-20% structural weight reduction, and 25% reduction in manufacturing cost compared to state-of-the-art riveted aluminum fuselage structures.

In 2020, the AATT project successfully formed four 10-ft. diameter by 6-ft. long Al 6061 ISCs in collaboration with Scot Forge and MT Aerospace. The ISCs were produced using the same mandrel from the 2019 forming campaign, producing 164, 0.5-inch tall longitudinal stiffeners with an average wall thickness between the stiffeners of 0.18-inch. One of the AATT ISCs is shown in Figure 15. The four 10-ft. diameter by 6-ft. long ISCs demonstrated excellent reproducibility. Among the four ISCs, the length varied by less than 1%, and the wall thickness varied less than 3% from the average of the four ISCs.

Figure 15. One of four, 10-ft. diameter by 6-ft. long, Al 6061 ISCs formed during the 2020 AATT forming campaign.

The four ISCs were heat treated to the T6 temper per AMS 2770 [11] after forming. This is the first time that multiple, commercial-scale ISCs have been heat treated to a T6 temper in a commercial production environment. Outer diameter and roundness measurements were made for each ISC after forming and after heat treatment to a T6 temper. This provided quantification of the dimensional quality of the as-formed part and the distortion associated with heat treatment. The results were reported as averages of individual measurements at multiple positions around the circumference at multiple locations along the length of the ISC.

The variation in average outer diameter versus height from the base of ISC are plotted in Figure 16 for each of the four ISCs. The desired as-formed profile is shown in gray along the y-axis to provide a visual representation of the outer mold line. The desired as-formed outer diameters at positions along the height of the cylinder consistent with the discrete physical measurement locations is plotted via the dashed black line as reference. The as-formed condition aligns well with the desired profile and is slightly oversized. Each of the four ISCs show similar trends in diameter both before and after heat treatment. In the as-formed condition, the diameter measurements for all ISCs four show good consistency at all locations along the length with the exception of the top section of the ISC.

It is noteworthy that the top region is left thicker intentionally to provide additional rigidity during forming to resist diametrical growth. Additionally, the roller travel at the top and bottom are limited by the machine design and the staggered nature of the rollers in the axial direction. Therefore, the top and bottom sections did not see uniform forming compared to the other locations along the length of the ISC. Hence, these factors contribute to increases in diameter compared to the fully-formed region with constant wall thickness. The diameter increased at all locations following heat treatment to the T6 condition, with the largest increases in diameter occurring near the ends of the ISC where the wall thickness is greatest.

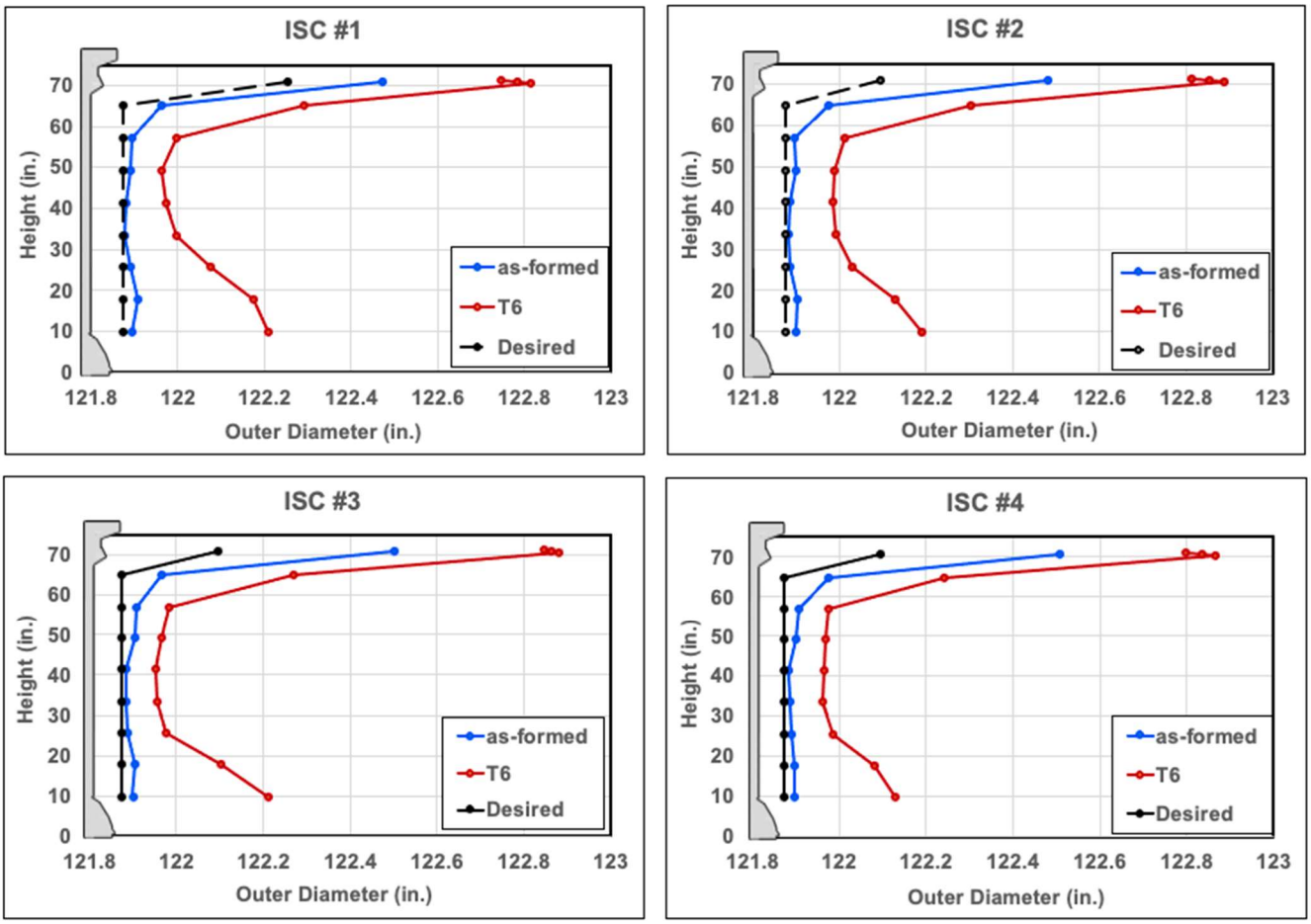

Figure 16. Plots of diameter versus height from base of ISC in the as-formed and heat treated (T6) conditions for each of the four AATT ISCs.

The deviation from the average outer diameter at each position along the length of the ISC was calculated and referred to as roundness. More specifically, the average diameter was calculated at each location along the ISC, and the deviation of each diameter measurement from the average was computed and averaged to determine roundness. The variation in roundness versus height from the base of the ISC are plotted in Figure 17 for each of the four ISCs. Again, the desired as-formed profile is shown in gray along the y-axis to provide a visual representation of the outer mold line. In the as-formed condition, deviation from roundness was generally very low (ranging from 0.05 to 0.2 inches across the four ISCs), indicating minimal deviation from an idealized perfect circular cross-section. This deviation increased following heat treatment to the T6 condition (ranging from 0.6 to 1.2 inches across the four ISCs), representing a maximum deviation of less than 1%. This low degree of roundness variation among these four ISCs is considered remarkable as this is such a new process. The degree of repeatability shown in retaining geometric consistency and tolerance in a production setting highlights the potential for this technology to be transitioned to industry for serial production.

Increased variability in roundness in the T6 condition is attributed to distortion after quenching and a slight increase in volume after aging. In ISCs #1 and #2, the increase in deviation from roundness was relatively constant along the length of the ISC. The greatest increases in deviation were found in the center of the fully formed regions in ISCs #3 and #4. It is unclear why the trend was different in the latter two ISCs. It is probable that these results can be improved upon with tooling and fixturing to minimize distortion during heat treatment and quenching. It is noteworthy

that these ISCs represent the first series of commercial-scale parts that have undergone heat treatment. Tooling and fixturing development will be one focus of further investigations aimed at maturing the process toward commercialization.

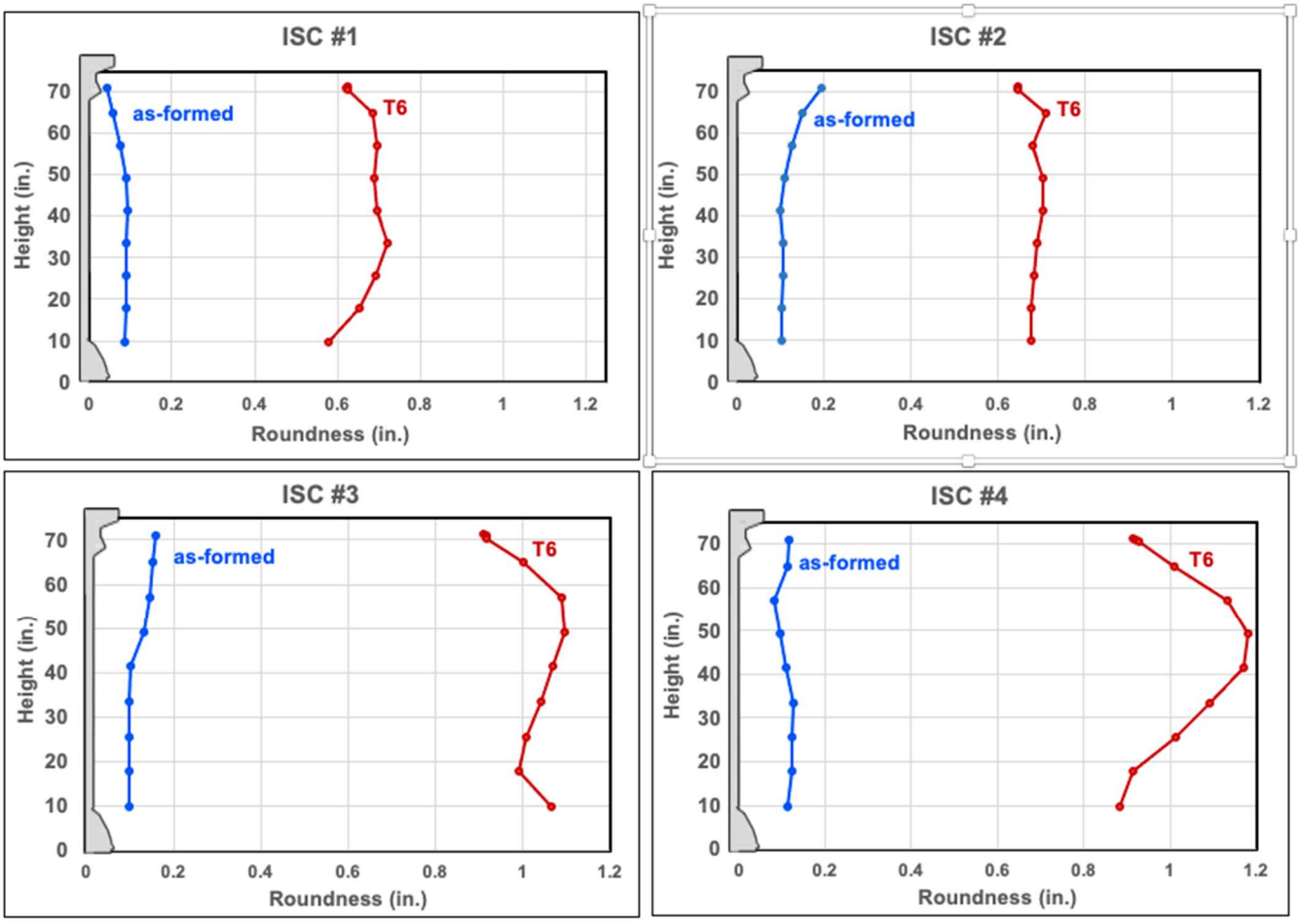

Figure 17. Plots of deviation from roundedness versus height from base of ISC in the as-formed and heat treated (T6) conditions for each of the four AATT ISCs.

The culmination of the AATT project is to assemble a metallic fuselage manufacturing demonstration article. In order to achieve this objective, the four ISCs will be joined via friction stir welding, followed by machining, and integrated with other support structure such as floors, circumferential structural frames, and window/door cutouts.

3.4 Mechanical Property Test Results for ISC Material

Mechanical testing of various ISCs was performed to quantify the mechanical properties of ISC products. Mechanical properties were measured in the fully processed, T6 temper that is anticipated to be representative of commercially-available product. The ISC materials were solution heat treated (SHT) and water quenched (WQ) after forming, followed by artificial aging to achieve a T6 temper. Cryotank barrel sections are typically used in a peak or near-peak aged T8 temper, which requires uniform plastic stretching prior to artificial aging. However, imparting consistent plastic deformation to a complex-shaped ISC will be difficult and require development of methods and tools to accomplish the task.

Development of the ISC process occurred primarily in the three aluminum alloys, 2219, 2050, and 6061. All three were evaluated in the fully-processed (solution heated treated, water

quenched, and aged to T6) state. The heat treatment parameters used to obtain a T6 temper for these alloys are provided in Table 7. The parameters were obtained from AMS 2770 [11] for 2219 and 6061. However, the T6 temper is not a standard commercial product for Al-Li alloy 2050. Hence, an internal aging study guided by consultation from the 2050 producer Constellium was undertaken to define the aging duration that led to the peak hardness. For aging at 330°F, the peak hardness in 2050 occurred at roughly 30 hours. This is consistent with the aging protocol to obtain a T6 temper for a similar Al-Li alloy, 2195.

Table 7. Heat treatment parameters aluminum alloys used in ISC forming.

Alloy	Heat treatment procedure for T6 temper	Ref. for Heat Treatment
2219	SHT 1 hr. at 995°F, WQ, Age 26 hr. at 375°F	AMS 2770 [11]
2050	SHT 1 hr. at 932°F, WQ, Age 30 hr. at 330°F	Constellium [13]
6061	SHT 1 hr. at 985°F, WQ, Age 9 hr. at 350°F	AMS 2770 [11]

*SHT = Solution heat treat; WQ = Water quench

Tensile tests were conducted in accordance with ASTM E8 [14] procedures using subscale, 4-inch-long dog-bone test specimens. Testing was conducted in two specimen orientations – axial and circumferential. Additionally, specimens were extracted from both the wall and stiffener regions of the ISC. Wall specimens were machined such that the center of the gauge section aligned with center of the wall between two adjacent stiffeners. Axial stiffener specimens were extracted from the center of the stiffener. Circumferential stiffener specimens were taken from the wall with the gauge section centered directly below the stiffener, due to limited material availability within the stiffener. Standard tensile properties, such as tensile yield strength (σ_y), ultimate tensile strength (σ_u), and elongation are reported based on the average of duplicate test specimens for each orientation and location. A list of available tensile test data for ISC material in a T6 temper is presented in Table 8. This includes properties for three alloys at the 10-ft. diameter scale and for Al 6061 at the sounding rocket scale. Typical and minimum properties for 6061-T6 are provided in Table 9 for comparison with other wrought product forms.

Table 8. Tensile test results for various Al alloys from ISCs.

Alloy-Temper Location	ISC Diameter	Orientation	σ_y (ksi)	σ_u (ksi)	Elongation (%)
2219-T6 Wall	120 inch Commercial Scale	Circumferential	43.3	59.0	15.7
		Axial	43.8	59.1	14.2
2050-T6 Wall	120 inch Commercial Scale	Circumferential	52.8	62.9	15.2
		Axial	54.1	64.0	10.2
6061-T6 Wall	120 inch Commercial Scale	Circumferential	45.3	48.6	6.4
		Axial	45.5	50.1	11.5
6061-T6 Stiffener	120 inch Commercial Scale	Circumferential	46.0	50.2	9.9
		Axial	46.3	50.4	30.3
6061-T6 Wall	17 inch Sounding Rocket	Circumferential	33.2	45.9	9.0
		Axial	43.0	46.3	9.8
6061-T6 Stiffener	17 inch Sounding Rocket	Circumferential	34.8	46.0	8.1
		Axial	42.5	46.6	11.9

Table 9. Reference tensile strengths of T6 products.

Reference T6 Data	σ_y (ksi)	σ_u (ksi)	Elongation (%)
2219 Wrought (typical) [15]	38	58	10.0
6061 Wrought (typical) [16]	40	45	14.5
6061 Wrought (minimum) [17]	35	42	9.0
2195 Wrought [13]	51-58	66-71	13-22

The sounding rocket test data displays some anisotropy in tensile yield strength between the axial and circumferential directions, with the circumferential direction roughly 8-10 ksi lower σ_y compared to the axial direction in both the stiffener and wall regions. The circumferential direction σ_y is slightly lower than minimum σ_y for Al 6061-T6 wrought product forms by 1-2 ksi. Meanwhile, the σ_u values for the circumferential direction meets or exceeds both the minimum and typical properties for Al 6061-T6. Elongation values were comparable with the reference wrought product minimum of 9%, with slightly lower elongation in the circumferential direction.

In the 10 ft. Al 6061 ISCs, properties were noticeably higher and more isotropic than those from the sounding rocket scale. Yield and ultimate strengths exceed typical T6 properties by ~10%. Elongation values in the wall are below the minimum reference values for wrought T6 products by approximately three percentage points in the circumferential direction. In contrast, the axial direction exceeded the referenced minimum by two percentage points. Excellent elongation was observed in the axial orientation of the stiffeners that far exceeded both minimum and typical properties.

Al 2219 and Al-Li 2050 tensile data is only available from the wall regions due to cracking in the stiffeners. The 10 ft. Al-Li 2050 ISC material provided superior strength properties compared to Al 6061 and Al 2219, as expected. Al 2219 properties were comparable to published wrought properties for T6 product forms. Since Al-Li 2050 is not commercially used in the T6 temper, there is no standard 2050-T6 data for comparison. Al-Li 2195, a similar alloy, was used instead for comparison with the Al-Li 2050 ISC data. Although Al-Li 2195 is infrequently used in the T6 temper condition, the Al-Li 2050 producer (Constellium) provided internal Al-Li 2195-T6 wrought product data for comparison as seen in Table 9 [13]. Values for the 2050 material are comparable with reported Al-Li 2195-T6 properties ranges. In summary, T6 properties for Al 6061, Al 2219 and Al-

Li 2050 indicate no detrimental impacts of the ISC process on mechanical behavior. At the 10 ft. scale, properties generally meet or exceed typical properties for similar T6 wrought product forms.

Fracture toughness data from compact tension specimens was acquired per ASTM Standard E1820 [14] in addition to tensile properties for the fully formed 6061 T6 ISC. These specimens were tested in two different orientations from the wall between stiffeners: axial-circumferential (A-C) and circumferential-axial (C-A). A specimen width of W = 2 inch was used. Table 10 shows average values for four specimens in each orientation along with handbook values for Al 6061-T6 wrought products. Fracture toughness was relatively isotropic in the ISC material. Toughness values were greater than 40 ksi-in^{½} in both orientations. Generally, the fracture toughness of the ISC was comparable to or exceeded the values for wrought Al 6061 products.

Table 10. Fracture toughness test results from 3-m (10-ft.) diameter Al 6061 ISC compared with other T6 commercial products.

6061-T6 Product Form	Orientation	K_{Ic} (ksi-in$^{1/2}$)
ISC	A-C	40.7
	C-A	43.0
Extrusion [18]	L-T	44.3
	T-L	30.3
Forged Plate [19]	In-plane 45°	36.2

3.5 Benefits of the ISC Process and Potential Applications

A cost-benefit analysis (CBA) study [20] was undertaken in 2015 by NASA to quantify the benefits of the ISC process over conventional, multi-piece welded construction for fabrication of cryogenic tank barrel sections. The CBA study obtained input regarding fabrication of cryotanks from 18 recognized experts within NASA and industry. A hypothetical tank size of 16-ft. in diameter by 20-ft. in length was selected for each fabrication method, as shown in Figure 18, which is within the size range of commercial launch vehicles in the US. The CBA showed that labor costs approach 60% of the total cost of construction using the conventional manufacturing approach.

The CBA study also estimated that the ISC process could reduce manufacturing cost by 50% compared to the conventional multi-piece approach. This reduction is due to reducing the manufacturing schedule by 40% through a reduction in labor hours for machining, welding, and inspection. Mass savings for the ISC process were estimated to range from 5-10% due to eliminating longitudinal welds and weld lands. Both cost and mass savings were confirmed in an independent internal CBA performed by MT Aerospace [1]. MT Aerospace and NASA demonstrated that the ISC process enables production of barrel with similar performance to orthogrid stiffened cylinders at the cost of smooth-wall barrels [1].

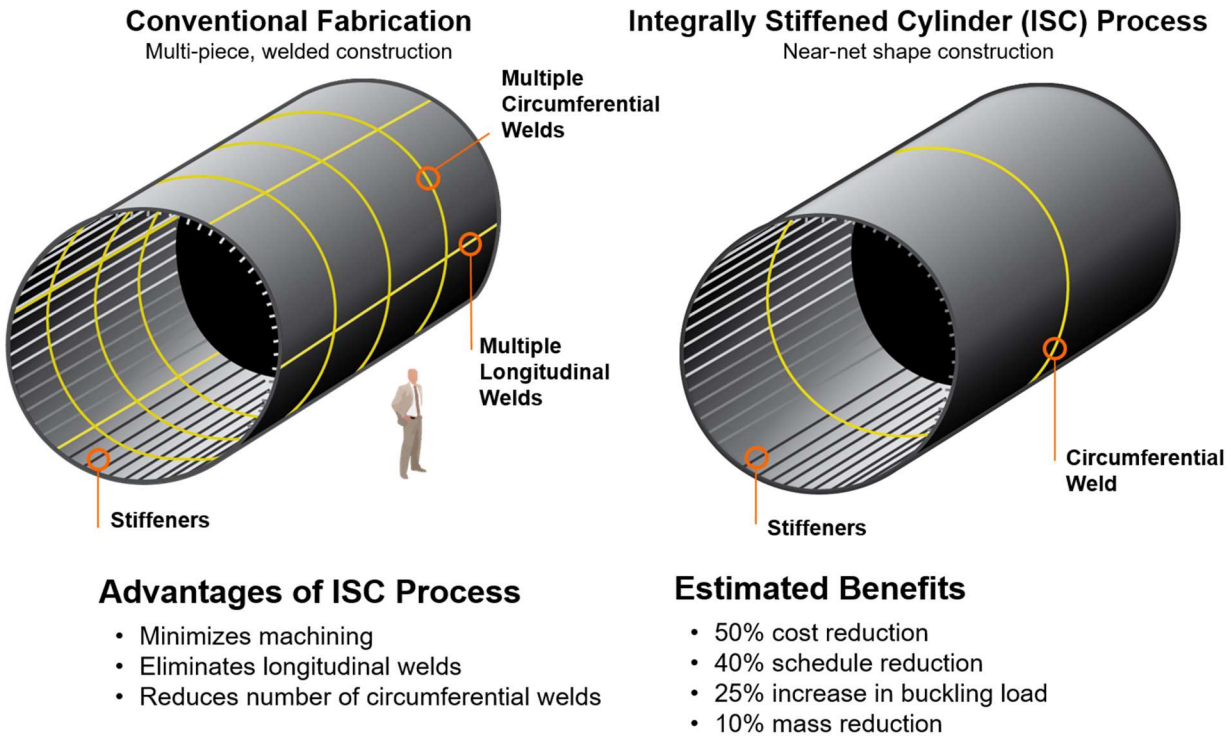

Figure 18. Advantages and benefits of the ISC process determined by the cost-benefit analysis study [20].

Further mass reduction is possible through design optimization, to capitalize on cryogenic tank designs enabled by the ISC process. As reported in section 3, structural testing of a single-piece, seamless, machined cylinder in the SBKF project showed a 28% increase in buckling load by eliminating longitudinal weld lands [2]. Structural design calculations estimate a similar magnitude increase in buckling performance for an ISC [1]. The increased buckling load capacity for an ISC is likely to be slightly lower due to the lack of stiffening in the circumferential direction, since the machined barrel test was for an orthogrid stiffened design and the ISC process currently only produces longitudinal stiffeners. It may be concluded from these analyses is an additional 5-10% mass savings is possible through design optimization, bringing the total estimated mass savings for ISC barrels to 10-20% compared to current multi-piece welded barrels.

The cost and schedule benefits noted for launch vehicles motivated the application of ISC technology for fuselage structure under the AATT project. This is in response to a US industry need for advanced concepts that reduce fuselage manufacturing time and cost relative to the traditional riveted assemblies. Initial structural design optimizations predict the use of ISCs can result in weight savings of more than 20% compared to incumbent single-aisle commercial aircraft. A thorough cost-benefit study is currently being conducted within the AATT project and will be reported separately.

4. Summary and Future Work

NASA has demonstrated two flow-forming solutions for large-scale single-piece, stiffened barrel production. One of these methods is commercially available and the other is nearing commercialization within US industry. The thick-walled and machined flow-formed barrels provide cost and mass savings associated with the elimination of longitudinal welding. By eliminating longitudinal welds, mass can be reduced by ~5% and has been verified to increase buckling load

by up to 28% compared to welded barrels. However, this approach still requires significant machining to convert the thick-wall barrel to a thin-walled barrel with internal stiffeners.

Over the past decade, the collaboration between NASA LaRC and MT Aerospace has resulted in developing the ISC process from proof-of-concept to a viable process at a commercially relevant scale. The process seeks to revolutionize the construction of aerospace hardware by producing single-piece structures that are lighter, cheaper, safer, and offer increased structural performance compared to traditional manufacturing methods. The ISC approach eliminates all longitudinal welds and greatly reduces the need for machining. The methodology is estimated to reduce costs by 50%, manufacturing schedule by 40%, and mass by ~10% compared to conventional multi-piece, welded construction. While a large-scale test has yet to be conducted, it is anticipated that a significant increase in buckling load (approaching 28%) is likely when compared to conventional multi-piece, welded construction. The ISC technology awaits successful infusion into aerospace markets by US industry. The technology has relevance for small-scale applications, such as sounding rockets and missiles, to large-scale applications, such as launch vehicles and aircraft fuselages.

5. Acknowledgments

The authors would like to acknowledge the support from several individuals and groups over the course of this work:

John Wagner (NASA LaRC - retired) for his efforts in near-net shape manufacturing technology development, cultivating external partnerships to support development of the ISC process, and his role in maturing the ISC process over the past decade.

Karen Taminger (NASA LaRC) for her support of the ISC work for aircraft applications within AATT.

Scot Forge and MT Aerospace for their assistance with contract management, production of ISC preforms, and performing ISC forming trials in recent years. Their partnership made the large-scale forming trials possible and were instrumental in the success demonstrated.

Sydney Newman (VA Tech) for her assistance as a student intern providing support for metallurgical analysis and mechanical testing of 10-ft. diameter ISC materials.

Harold (“Clay”) Claytor and James Baughman (Analytical Mechanics and Associates) for support with metallurgical analysis and heat treatment.

6. References

[1] D. Zell, M. Domack, W. Tayon, M. Stachulla, and J. Wagner, “Developments on Low Cost Manufacturing Methods for Cylindrical Launch Vehicle Structures,” presented at the 67th International Astronautical Congress, 2019.

[2] M. T. Rudd, M. W. Hilbsurger, A. E. Lovejoy, M. C. Lindell, N. W. Gardner, and M. R. Schultz, “Buckling response of a large-scale, seamless, orthogrid-stiffened metallic cylinder,” presented at the 2018 AIAA/ASCE/AHS/ASC Structures, Structural Dynamics, and Materials Conference, 2018, p. 1987.

[3] R. P. Thornburgh and M. W. Hilbsurger, “Longitudinal Weld Land Buckling in Compression-Loaded Orthogrid Cylinders,” *NASA Technical Memorandum*, NASA/TM-2010-216876, ARL-TR-5121, 2010.

[4] P. Murphy, J. Falker, K. Earle, M. Cirillo, and D. Reeves, “STMD’s New Strategic Framework Update,” *National Aeronautics and Space Administration. www.nasa.gov/spacetech*, 2017.

[5] “NASA FY19 Budget Request,” 2019. https://www.nasa.gov/content/fy-2019-budget.

[6] J. G. Sessler and V. Weiss, Eds., *Aerospace Structural Metals Handbook*. Syracuse University Press, 1967.

[7] “Aerospace Material Specification 4144: Aluminum Alloy, Hand Forgings and Rolled Rings,” SAE International, Warrendale, PA, 2020.

[8] “Aerospace Material Specification 4295B: Aluminum Alloy, Sheet and Plate,” SAE International, Warrendale, PA, 2006.

[9] “Metallic Materials Properties Development and Standardization (MMPDS-15),” Battelle Memorial Institute, 2020.

[10] “Military Handbook - MIL-HDBK-5H: Metallic Materials and Elements for Aerospace Vehicle Structures,” U.S. Department of Defense, 1998.

[11] “Aerospace Material Specification 2770H: Heat Treatment of Wrought Alumunum Alloy Parts,” SAE International, Warrendale, PA, 2010.

[12] W. Tayon, M. Domack, and J. Wagner, “Characterization of 10-ft. Diameter, Aluminum Alloy 2219 Integrally Stiffened Cylinders,” 2019.

[13] “Personal Communication with Constellium Regarding Al-Li Alloy 2195-T6 Properties,” 2018.

[14] “Annual Book of ASTM Standards Vol. 3.01,” American Society for Testing and Materials, West Conshohocken, PA, 2010.

[15] “Aerospace Materials Specification (AMS) 4143E: Aluminum Alloy Forgings and Rolled or Forged Rings 6.3Cu - 0.30Mn - 0.18Zr - 0.10V - 0.06Ti (2219-T6) Solution and Precipitation Heat Treated,” SAE International, Warrendale, PA, 2007.

[16] “Al 6061-T6 Material Data Sheet,” 2021. http://www.matweb.com/search/datasheet.aspx?MatGUID=b8d536e0b9b54bd7b69e4124d8f1d20a.

[17] “Aerospace Metals Specification AMS 4127 Rev. K: Aluminum Alloy, Forgings and Rolled or Forged Rings, (6061-T6) Solution and Precipitation Heat Treated,” SAE International, Warrendale, PA, 2019.

[18] F. J. MacMaster, K. S. Chan, S. C. Bergsma, and M. E. Kassner, “Aluminum alloy 6069 part II: fracture toughness of 6061-T6 and 6069-T6,” *Materials Science and Engineering: A*, vol. 289, no. 1–2, pp. 54–59, 2000.

[19] M. Nakai and G. Itoh, “The effect of microstructure on mechanical properties of forged 6061 aluminum alloy,” *Materials Transactions*, vol. 55, no. 1, pp. 114–119, 2014.

[20] M. C. Stoner, A. R. Hehir, M. L. Ivanco, and M. S. Domack, “Cost-Benefit Analysis for the Advanced Near Net Shape Technology (ANNST) Method for Fabricating Stiffened Cylinders,” *NASA Technical Memorandum*, NASA/TM–2016-219192, 2016.

REPORT DOCUMENTATION PAGE

Form Approved
OMB No. 0704-0188

1. REPORT DATE *(DD-MM-YYYY)*	2. REPORT TYPE	3. DATES COVERED *(From - To)*
01/01/2022	TECHNICAL MEMORANDUM	

4. TITLE AND SUBTITLE
Development of Advanced Manufacturing Approaches for Single-Piece Launch Vehicle Structures

5a. CONTRACT NUMBER

5b. GRANT NUMBER

5c. PROGRAM ELEMENT NUMBER

6. AUTHOR(S)
Wesley A. Tayon, Marcia S. Domack, Mark W. Hilburger
NASA Langley Research Center

Michelle T. Rudd
NASA Marshall Space Flight Center

5d. PROJECT NUMBER

5e. TASK NUMBER

5f. WORK UNIT NUMBER
081876.02.07.50.15.01.04

7. PERFORMING ORGANIZATION NAME(S) AND ADDRESS(ES)
NASA Langley Research Center
Hampton, VA 23681-2199

8. PERFORMING ORGANIZATION REPORT NUMBER

9. SPONSORING/MONITORING AGENCY NAME(S) AND ADDRESS(ES)
National Aeronautics and Space Administration
Washington, DC 20546-001

10. SPONSOR/MONITOR'S ACRONYM(S)
NASA

11. SPONSOR/MONITOR'S REPORT NUMBER(S)
NASA/TM-20210026743

12. DISTRIBUTION/AVAILABILITY STATEMENT
Unclassified - Unlimited
Subject Category
Availability: NASA STI Program (757) 864-9658

13. SUPPLEMENTARY NOTES

14. ABSTRACT

Advanced, near-net shape manufacturing methods have the potential to enable production of structures with fewer welds and reduced machining requirements. Two such methods that are suitable for the manufacturing of single-piece, stiffened barrel-shaped structures are presented.

15. SUBJECT TERMS
machining; flow-forming; integrally stiffened cylinder

16. SECURITY CLASSIFICATION OF:			17. LIMITATION OF ABSTRACT	18. NUMBER OF PAGES	19a. NAME OF RESPONSIBLE PERSON
a. REPORT	b. ABSTRACT	c. THIS PAGE			HQ - STI-infodesk@mail.nasa.gov
U	U	U	UU	29	19b. TELEPHONE NUMBER *(Include area code)* 757-864-9658